J|A|C|S
ARTICLES
Published on Web 01/24/2007

Cross-Linking of Cationic Block Copolymer Micelles by Silica Deposition

Jian-Jun Yuan, Oleksandr O. Mykhaylyk, Anthony J. Ryan, and Steven P. Armes*

Contribution from the Department of Chemistry, The University of Sheffield, Brook Hill, Sheffield S3 7HF, United Kingdom

Received October 26, 2006; E-mail: s.p.armes@sheffield.ac.uk

Abstract: Diblock copolymer micelles comprising cationic poly(2-(dimethylamino)ethyl methacrylate) (PDMA) coronas and hydrophobic poly(2-(diisopropylamino)ethyl methacrylate) (PDPA) cores are used as nanosized templates for the deposition of silica from aqueous solution at pH 7.2 and 20 °C. Both noncross-linked and shell cross-linked (SCL) micelles can be coated with silica without loss of colloid stability. Under optimized conditions, the silica deposition is confined to the partially quaternized cationic PDMA chains, leading to hybrid copolymer−silica particles of around 35 nm diameter with well-defined core−shell morphologies. ^{1}H NMR studies confirmed that the PDPA cores of these copolymer−silica particles became protonated at low pH and deprotonated at high pH, which suggests possible encapsulation and controlled release applications. Moreover, in situ silica deposition effectively stabilizes the PDPA−PDMA micelles, which remain intact on lowering the solution pH (whereas the original noncross-linked PDPA−PDMA micelles dissociate in acidic solution). This suggests a convenient route to silica-stabilized SCL micelles under mild conditions.

Biomineralization of silica, or biosilicification, occurs in water under ambient conditions for various biological systems such as diatoms and sponges. Moreover, this natural process leads to exquisite hierarchical structures and multiple morphologies with precise nanoscale control, which continues to elude materials scientists.[1] Ideally, any biomimetic approach to silica synthesis would be both environmentally benign and also highly controllable for generating a range of structures and morphologies. Drawing on our recently improved understanding of biosilicification,[2] numerous studies have successfully demonstrated silica formation under ambient conditions.[3] In contrast, morphological and structural control remains a major long-term challenge. By screening series of long-chain amines or polypeptides or by applying external fields, complex silica structures such as hexagonal, plate/sheetlike (or aligned platelets) fibers or dendrites have been reported.[4] Alternatively, synthesis of "designer" silicas has been achieved by designing polyamines with various architectures that are subsequently self-assembled into well-defined aggregates to act as functional templates for silica deposition. For example, using poly(ethylene imine) stars as templates leads to markedly different silica morphologies compared to linear chains.[5]

It is well-known that block copolymers can self-assemble into a wide range of nanostructures that can be used for controlling the formation of various inorganic materials.[6] However, block copolymer-mediated silica formation is seldom reported.[7,8] Deming and co-workers[7] have reported that block copolypeptides self-assemble into structured aggregates that facilitate silica deposition under ambient conditions and simultaneously direct silica morphologies on micrometer length scales. Very recently, Shantz and co-workers[8] described using polypeptide-based vesicles as templates for the formation of hollow silica spheres. There are many literature examples of nanostructured inorganic oxide particles,[9−11] but in many cases these are hollow particles produced by either calcination or by either chemical or physical degradation of the core template. For example, a very recent report describes the preparation of micrometer-sized hollow silica particles via the in situ physical removal of a polystyrene latex template.[10] However, such approaches are inherently inefficient, and the loading of these hollow particles with appropriate actives can be problematic. Nevertheless, there is still considerable interest in developing facile routes to nano-

(1) Müller, W. E. G. Silicon Biomineralization: Biology-Biochemistry-Molecular Biology-Biotechnology; Springer: Berlin, 2003.
(2) (a) Shimizu, K.; Cha, J.; Stucky, G. D.; Morse, D. E. *Proc. Natl. Acad. Sci. U.S.A.* **1998**, *95*, 6234−6238. (b) Kröger, N.; Deutzmann, R.; Sumper, M. *Science* **1999**, *286*, 1129−1132. (c) Cha, J. N.; Shimizu, K.; Zhou, Y.; Christiansen, S. C.; Chmelka, B. F.; Stucky G. D.; Morse D. E. *Proc. Natl. Acad. Sci. U.S.A.* **1999**, *96*, 361−365. (d) Poulsen, N.; Sumper, M.; Kröger, N. *Proc. Natl. Acad. Sci. U.S.A.* **2003**, *100*, 12075−12080.
(3) Patwardhan, S. V.; Clarson, S. J.; Perry, C. C. *Chem. Commun.* **2005**, 1113−1121.
(4) (a) Bellomo, E. G.; Deming, T. J. *J. Am. Chem. Soc.* **2006**, *128*, 2276−2279. (b) Tomczak, M. M.; Glawe, D. D.; Drummy, L. F.; Lawrence, C. G.; Stone, M. O.; Perry, C. C.; Pochan, D. J.; Deming, T. J.; Naik, R. R. *J. Am. Chem. Soc.* **2005**, *127*, 12577−12582. (c) Yuan, J. J.; Zhu, P. X.; Fukasawa, N.; Jin, R. H. *Adv. Funct. Mater.* **2006**, *16*, 2202−2212. (d) Yuan, J. J.; Jin, R. H. *Adv. Mater.* **2005**, *17*, 885−888. (e) Rodriguez, F.; Glawe, D. D.; Naik, R. R.; Hallinan, K. P.; Stone, M. O. *Biomacromolecules* **2004**, *5*, 261−265. (f) Naik, R. R.; Whitlock, P. W.; Rodriguez, F.; Brott, L. L.; Glawe, D. D.; Clarson, S. J.; Stone, M. O. *Chem. Commun.* **2003**, 238−239. (g) Patwardhan, S. V.; Mukherjee, N.; Steinitz-Kannan, M.; Clarson, S. J. *Chem. Commun.* **2003**, 1122−1123.
(5) Jin, R. H.; Yuan, J. J. *Chem. Commun.* **2005**, 1399−1401.
(6) (a) Lazzari, M.; López-Quintela, M. A. *Adv. Mater.* **2003**, *15*, 1583−1594. (b) Föster, S.; Antonietti, M. *Adv. Mater.* **1998**, *10*, 195−217.
(7) Cha, J. N.; Stucky, G. D.; Morse, D. E.; Deming, T. J. *Nature* **2000**, *403*, 289−292.
(8) Jan, J.-S.; Lee, S.; Carr, C. S.; Shantz, D. F. *Chem. Mater.* **2005**, *17*, 4310−4317.
(9) Caruso, F. *Chem.−Eur. J.* **2000**, *6*, 413−419.
(10) Chen, M.; Wu, L.; Zhou, S.; You, B. *Adv. Mater.* **2006**, *18*, 801−806.
(11) Schmid, A.; Fujii, S.; Armes, S. P. *Langmuir* **2006**, *22*, 4923−4927.

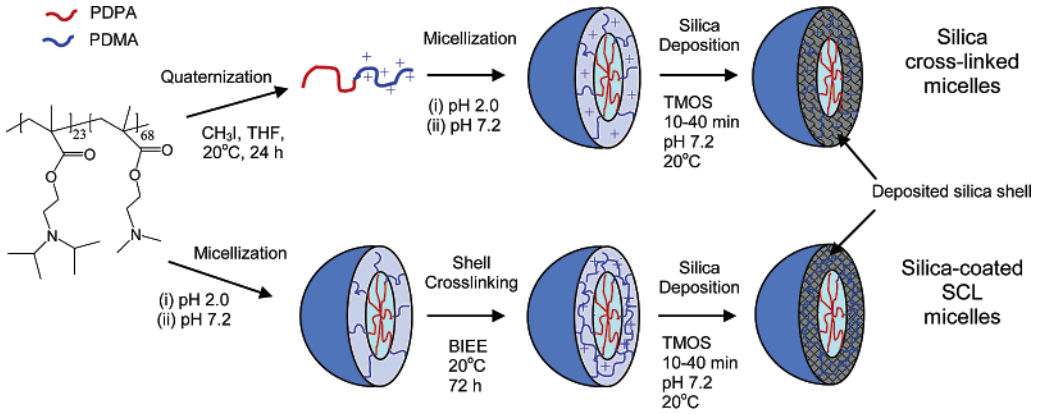

Figure 1. Schematic formation of hybrid copolymer−silica particles obtained by the in situ hydrolysis of tetramethyl orthosilicate (TMOS) using cationic block copolymer micelles as templates. Using either noncross-linked micelles (upper route) or shell cross-linked micelles (lower route) produces hybrid copolymer−silica particles with well-defined core−shell morphologies (the PDPA block is located within the core, while the shell comprises both silica and the PDMA chains); the upper route also leads to silica cross-linking of the micelles.

structured inorganic particles, since silica and other inorganic oxides such as calcium carbonate should offer more effective diffusional barriers for encapsulated actives (drugs, fragrances, pesticides. etc.) than relatively porous organic/polymer layers. Indeed, Huo et al. recently reported the use of block copolymer micelles based on a nonionic Pluronic block copolymer to template silica deposition, albeit under rather acidic conditions.[12] The uptake and release of various drugs and dyes from the resulting nanoparticles was studied using fluorescence techniques and confocal microscopy, and the silica shells appear to retard diffusional release rates, as expected.

Herein we examine the use of both noncross-linked and shell cross-linked (SCL) micelles based on a tertiary amine methacrylate-based block copolymer, namely poly(2-(diisopropylamino)ethyl methacrylate)-*block*-2-(dimethylamino)ethyl methacrylate (or $PDPA_{23}$−$PDMA_{68}$, where the subscripts denote the mean degrees of polymerization of each block; see Figure 1, Supporting Information, and refs 15−20), as templates for the formation of well-defined hybrid copolymer−silica particles of less than 50 nm diameter.

Results and Discussion

The synthesis of tertiary amine methacrylate-based diblock copolymers over a range of block compositions and copolymer molecular weights can be achieved using either group transfer polymerization[13] or controlled radical polymerization.[21] More specifically, PDPA−PDMA diblock copolymers dissolve molecularly in acidic solution as cationic polyelectrolytes due to protonation of both polyamine blocks. On adjusting the solution pH with aqueous base, micellar self-assembly occurs at around neutral pH; the deprotonated hydrophobic PDPA chains form the micelle cores, and the cationic (protonated) PDMA chains form the micelle coronas.[13c] Shell cross-linking of these micelles can be readily achieved at high dilution using 1,2-bis(2-iodoethoxy)ethane (BIEE) as a bifunctional reagent under mild conditions.[14] BIEE quaternizes the PDMA chains selectively, since the PDPA chains are much less reactive.[13c,14b] Our synthetic strategy is shown in Figure 1. The PDMA shell has significant cationic character due to either protonation and/or quaternization, so it can act both as a polymeric catalyst under mild conditions[22] and also as a physical scaffold for silica deposition. Tetramethoxysilane (TMOS) was employed as a silica precursor, and silica deposition was conducted in aqueous solution at 20 °C at around neutral pH.

Silica-based core−shell nanoparticles have been suggested for various bioanalytical applications such as drug delivery, bioimaging, and biolabeling.[23] Such particles have been previously synthesized by coating functional cores with silica shells using either Stöber chemistry[24] or by employing a microemulsion approach.[25] Both methods require nonideal conditions, such as elevated temperature, nonphysiological pH, and the presence of either large amounts of surfactants and/or organic cosolvents. In contrast, our syntheses of core−shell nanoparticles are conducted in aqueous solution at ambient temperature and neutral pH, while maintaining good control over both the particle morphology and colloid stability. These conditions are considerably more benign than those employed by Huo et al.,[12] since

(12) Huo, Q.; Liu, J.; Wang, L.-Q.; Jiang, Y.; Lambert, T. N.; Fang, E. *J. Am. Chem. Soc.* **2006**, *128*, 6447−6453.
(13) (a) Bütün, V.; Billingham, N. C.; Armes, S. P. *Chem. Commun.* **1997**, 671−672. (b) Bütün, V.; Billingham, N. C.; Armes, S. P. *Polymer* **2001**, *42*, 5993−6008. (c) Bütün, V.; Armes, S. P.; Billingham, N. C. *Macromolecules* **2001**, *34*, 1148−1159.
(14) (a) Liu, S.; Armes, S. P. *J. Am. Chem. Soc.* **2001**; *123*, 9910−9911. (b) Bütün, V.; Billingham, N. C.; Armes, S. P. *J. Am. Chem. Soc.* **1998**, *120*, 12135−12136.
(15) Svergun, D. I. *J. Appl. Crystallogr.* **1992**, *25*, 495−503.
(16) Svergun, D. I.; Semenyuk, A. V.; Feigin, L. A. *Acta Crystallogr., Sect. A* **1988**, *44*, 244−250.
(17) Griffiths, T. R.; Nerukh, D. A.; Eremenko, S. A. *Phys. Chem. Chem. Phys.* **1999**, *1*, 3199−3208.
(18) Nerukh, D. A. Dyefe-Dynamic Equation Fitting Engine, 2003, http://www.chem. pwf.cam.ac.uk/~dn232/software/dyefe/index.html.
(19) Glatter, O. J. *Appl. Crystallogr.* **1979**, *12*, 166−175.
(20) Bolze, J.; Ballauff, M.; Kijlstra, J.; Rudhardt, D. *Macromol. Mater. Eng.* **2003**, *288*, 495−502.
(21) Liu, S.; Weaver, J. V. M.; Tang, Y.; Billingham, N. C.; Armes, S. P.; Tribe, K. *Macromolecules* **2002**, *35*, 6121−6131.
(22) (a) Jia, Y.; Gray, G. M.; Hay, J. N.; Li, Y.; Unali, G.-F.; Baines, F. L.; Armes, S. P. *J. Mater. Chem.* **2005**, *15*, 2202−2209. (b) Kim, D. J.; Lee, K. B.; Chi, Y. S.; Kim, W. J.; Paik, H. J.; Chio, I. S. *Langmuir* **2004**, *20*, 7904−7906.
(23) (a) Tan, W.; Wang, K.; He, X.; Zhao, X. J.; Drake, T.; Wang, L.; Bagwe, R. P. *Med. Res. Rev.* **2004**, *24*, 621−638. (b) Mulvaney, P.; Liz-Marzan, L. M.; Giersig, M.; Ung, T. J. *Mater. Chem.* **2000**, *10*, 1259−1270.
(24) (a) Nann, T.; Mulvaney, P. *Angew. Chem., Int. Ed.* **2004**, *43*, 5393−5396. (b) Schroedter, A.; Weller, H.; Eritja, R.; Ford, W. E.; Wessels, J. M. *Nano Lett.* **2002**, *2*, 1363−1367.
(25) (a) Darbandi, M.; Thomann, R.; Nann, T. *Chem. Mater.* **2005**, *17*, 5720−5725. (b) Santra, S.; Yang, H.; Holloway, P. H.; Stanley, J. T.; Mericle, R. A. *J. Am. Chem. Soc.* **2005**, *127*, 1656−1657. (c) Yi, D. K.; Selvan, S. T.; Lee, S. S.; Papaefthymiou, G. C.; Kundaliya, D.; Ying, J. Y. *J. Am. Chem. Soc.* **2005**, *127*, 4990−4991. (d) Santra, S.; Tapec, R.; Theodoropoulou, N.; Dobson, J.; Hebard, A.; Tan, W. *Langmuir* **2001**, *17*, 2900−2906.

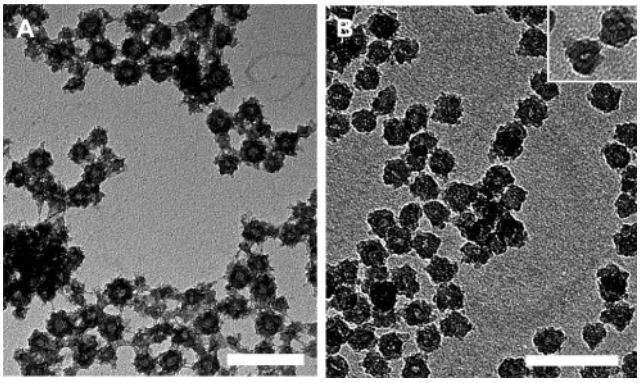

Figure 2. TEM images of hybrid copolymer−silica particles: (A) synthesized using nonquaternized $PDPA_{23}$−$PDMA_{68}$ copolymer micelles as templates; (B) synthesized using partially quaternized noncross-linked copolymer micelles (50% with respect to the PDMA shell). The inset in (B) is a typical high magnification image obtained after dispersing these particles directly into an acidic solution (pH 2); this confirms that silica deposition cross-links and stabilizes the micelles, which would otherwise dissociate at low pH. The scale bars are 100 nm in each case.

we employ *cationic* block copolymer micelles as colloidal templates to promote *localized* silica deposition.

In our preliminary experiments we used conventional (noncross-linked) micelles prepared directly from the $PDPA_{23}$−$PDMA_{68}$ diblock copolymer precursor. Dynamic light scattering (DLS) studies indicated an intensity-average micelle diameter of 37 nm at 25 °C. At pH 7.2 the PDMA chains in the micelle corona are approximately 50% protonated, so they have appreciable cationic character.[13b] Silicification was achieved simply by mixing 2.0 mL of an aqueous copolymer micelle solution (0.25 w/v % at pH 7.2) with 1.0 mL of TMOS at 20 °C for 20 min. Thermogravimetric analyses indicated that the mean diblock copolymer content of the copolymer−silica particles was about 15% by mass. Figure 2A shows a typical TEM image obtained for these TMOS-treated micelles. The formation of copolymer−silica particles with well-defined core−shell morphologies is readily confirmed, since the silica/PDMA hybrid shell is more electron-dense than the PDPA chains within the micelle cores. These particles have a number-average diameter of around 35 nm, which is in reasonably good agreement with the dimensions of the precursor micelles. However, in addition to the formation of these copolymer−silica particles, some ill-defined, nontemplated silica structures are also observed in Figure 2A, indicating that the silica formation is not particularly well controlled in this case. Ideally, silica deposition should occur exclusively on the cationic copolymer micelles, rather than in bulk solution.

A set of simple comparative experiments indicated possible approaches to improve our control over the silica deposition. On mixing 1.0 mL of TMOS and 1.0 mL of aqueous PDMA *homopolymer* solution (concentration of DMA repeat units, [DMA] = 0.064 M) at pH 7.2 and 20 °C, the initially heterogeneous solution became homogeneous after continuous stirring for 15 min.[26] In comparison, for 50% and 100% quaternized PDMA *homopolymers* under identical conditions, the corresponding times required for the reaction solutions to become homogeneous were 25 and 50 min, respectively. This suggests that quaternized PDMA chains catalyze slower (and hence perhaps more controlled) hydrolysis of the TMOS precursor. These control experiments suggested that well-controlled silica deposition might be achieved using (partially) quaternized $PDPA_{23}$−$PDMA_{68}$ copolymer micelles as templates. First, selective quaternization of the DMA residues was achieved using methyl iodide under mild conditions.[13c] A 0.25 wt% aqueous solution of $PDPA_{23}$−$PDMA_{68}$ diblock copolymer micelles in which the PDMA chains were 50% quaternized had an intensity-average diameter of 29 nm at pH 7.2, as indicated by DLS. TMOS (1.0 mL) was added to 2.0 mL of this aqueous micelle solution at 20 °C, and silica deposition continued for 20 min with continuous stirring prior to isolation via centrifugation. TEM images of the purified hybrid copolymer−silica particles are shown in Figure 2B. Core−shell nanostructures were clearly observed, with a number-average diameter of 28 nm. DLS studies indicated an intensity-average diameter of 34 nm. In contrast to the nonquaternized diblock precursor, there was no evidence for nontemplated silica structures, suggesting that secondary nucleation had been minimized by using this partially quaternized copolymer. Similar results were obtained using micelles with 100% quaternized PDMA blocks (see Figure S1). Thermogravimetric analyses indicated that the mean diblock copolymer contents of the copolymer−silica particles derived from micelles with 50% and 100% quaternized PDMA blocks were about 18% and 16% by mass, respectively. Thus quaternization of the PDMA chains appears to be beneficial for well-controlled silica deposition. Moreover, these quaternized micelles produced copolymer−silica particles with thicker silica shells relative to those obtained using nonquaternized copolymer micelles (see Figure 2A) under the same conditions.

Furthermore, we found that the nanostructure of these silica particles could be simply controlled by tuning the amount of TMOS used for silica deposition. For example, silica particles with relatively thin shells and large cores were obtained when using lower levels of TMOS. As shown in Figure 3A, well-defined silica particles with a number-average diameter of around 26 nm were formed by stirring a mixture of 58 mg of TMOS with 2 mL of a 0.25 w/v % solution of 50% quaternized copolymer micelles for 20 min. Thermogravimetric analysis indicated that the mean copolymer content of these hybrid copolymer−silica particles was about 28% by mass, indicating a silica conversion of about 58%. Moreover, colloidal stability was maintained even after the reaction time was increased from 20 min to 8 h when using this reduced amount of TMOS (see Figure 3B). Again, there is no evidence for nontemplated silica (such as that observed in Figure 2B), indicating efficient templating of these silica nanostructures.

It is worth emphasizing that silica deposition effectively cross-links the copolymer chains and stabilizes the micelles with respect to dissociation. DLS studies on the silica-coated micelles obtained using the 50% quaternized copolymer precursor indicated an intensity-average micelle diameter of 34.0 nm at around pH 7. Almost the same intensity-average micelle diameter (33.5 nm) was obtained at pH 2, whereas the noncross-linked precursor micelles dissociated completely in acidic solution. TEM studies provided further evidence of efficient micelle cross-linking via silica deposition. As shown in Figure 2B (see inset) and Figure S2, the silica cross-linked micelles retain their core−shell morphology after direct dispersion and drying at pH 2. ^{1}H NMR studies of the hybrid copolymer−

(26) Hydrolysis of TMOS produces a homogeneous aqueous solution of silicic acid.

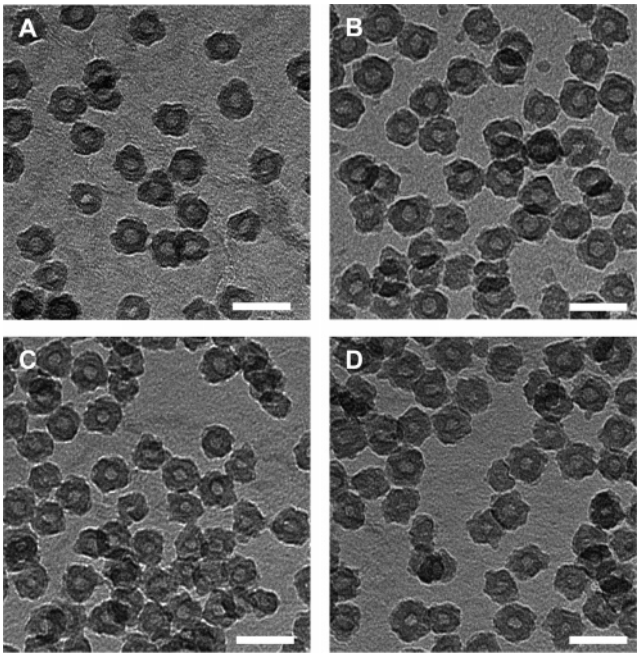

Figure 3. TEM images obtained for hybrid copolymer−silica particles with well-defined core−shell morphologies synthesized by using partially quaternized $PDPA_{23}$−$PDMA_{68}$ copolymer micelles (50% with respect to the PDMA shell) as templates: (A) prepared by stirring a mixture of 2.0 mL of a 0.25 w/v % copolymer micelle solution with 58 mg TMOS for 20 min; (B) silica deposition conducted for 8 h using the same conditions as those employed in (A); (C) prepared by stirring a mixture of 1.0 mL of a 1.0 w/v % copolymer micelle solution with 116 mg of TMOS for 20 min; (D) prepared by stirring a mixture of 1.0 mL of a 2.0 w/v % copolymer micelle solution with 232 mg of TMOS for 20 min. The scale bars are 50 nm in each case.

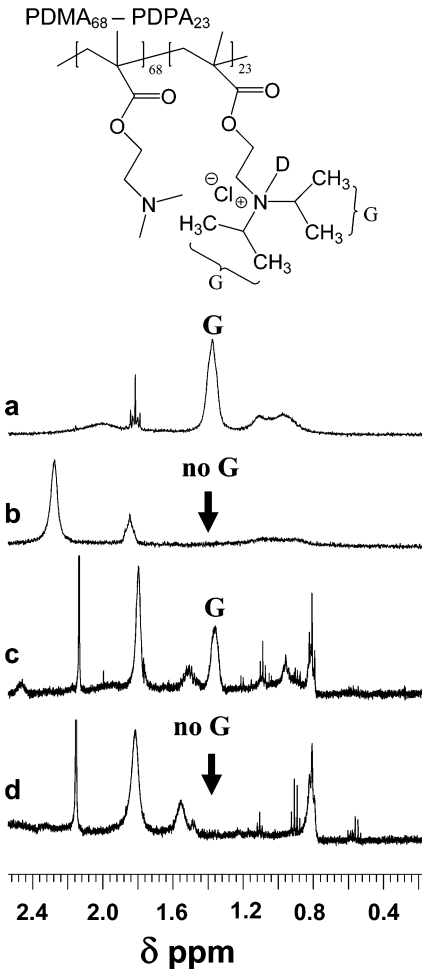

Figure 4. ^{1}H NMR spectra of the following: (a) a molecular solution of the $PDPA_{23}$−$PDMA_{68}$ diblock copolymer (50% quaternized PDMA block using methyl iodide) in D_2O/DCl at pH 2 (signal G at δ 1.3−1.4 is due to the four equivalent methyl groups of the protonated DPA residues); (b) micelles for the same copolymer obtained in D_2O at pH 7 (there is no longer a G signal at δ 1.3−1.4 due to the DPA residues since the PDPA block becomes deprotonated and forms hydrophobic micelle cores at this pH); (c) copolymer−silica particles derived from $PDPA_{23}$−$PDMA_{68}$ diblock copolymer micelles (50% quaternized PDMA block) in DCl/D_2O at pH 2 (the signal G at δ 1.3−1.4 corresponds to the protonated PDPA chains within the micelle cores); (d) the same copolymer−silica particles in D_2O at pH 7 (signal G at δ 1.3−1.4 disappears, indicating that the PDPA chains in the micelle cores become hydrophobic due to deprotonation).

silica particles dispersed in DCl/D_2O at pH 2 revealed a signal at δ 1.3−1.4 due to the protonated PDPA chains (see Figure 4). When the solution pH was increased to pH 7 by addition of NaOD, this signal disappeared as the PDPA chains became deprotonated and hence hydrophobic. Thus these spectroscopic studies confirmed that the PDPA chains in the micelle cores are both accessible and pH-responsive (i.e., they can become hydrophilic at low pH and hydrophobic at high pH) which suggests possible encapsulation/controlled release applications for these new hybrid copolymer−silica particles.

SCL micelles are an emerging new class of nanoparticles for which various potential applications such as targeted drug delivery, solubilization, catalysis, fillers, and coatings have been suggested.[27] The synthesis of SCL micelles usually involves covalent stabilization of the micelle coronal chains,[27] although polyion cross-linking has also been recently suggested.[28] Typically, shell cross-linking is conducted at high dilution (normally less than 0.5 wt.% copolymer micelles) in order to avoid intermicelle fusion.[27] However, silica cross-linked micelles can be synthesized at somewhat higher concentrations. As shown in Figure 3C, mixing a 1.0 mL solution of 1.0 w/v % copolymer micelles (50% quaternized with respect to the PDMA shell) with 116 mg of TMOS for 20 min produced hybrid copolymer−silica particles of about 26 nm with well-defined core−shell morphologies. Similar-sized particles were also obtained using 2.0 w/v % copolymer micelles (see Figure 3D). Thermogravimetric analyses indicated that the mean copolymer contents of the hybrid copolymer−silica particles shown in Figure 3C and 3D were about 20 and 22% by mass, respectively, with corresponding silica conversions of 87 and 78%. Thus the synthesis of SCL micelles by silica deposition can be rather efficient under appropriate conditions. Given the mild conditions, fast reaction times, and relatively cheap reagents employed, such "inorganic" cross-linking appears to offer some advantages over conventional covalent cross-linking. Moreover, the final hybrid copolymer−silica particles are expected to be reasonably biocompatible, and the inorganic shell is expected to offer a more effective diffusional barrier for the long-term entrapment of hydrophobic additives within the micelle cores. Mann and co-workers have recently reported coating *preformed* SCL micelles with calcium phosphate.[29] However, as far as we are aware, there is only one literature report that describes

(27) Wooley, K. L. *J. Polym. Sci., Part A: Polym. Chem.* **2000**, *38*, 1397−1407.
(28) Weaver, J. V. M.; Tang, Y.; Liu, S.; Iddon, P. D.; Grigg, R.; Billingham, N. C.; Armes, S. P.; Hunter, R.; Rannard, S. P. *Angew. Chem., Int. Ed.* **2004**, *43*, 1389−1392.

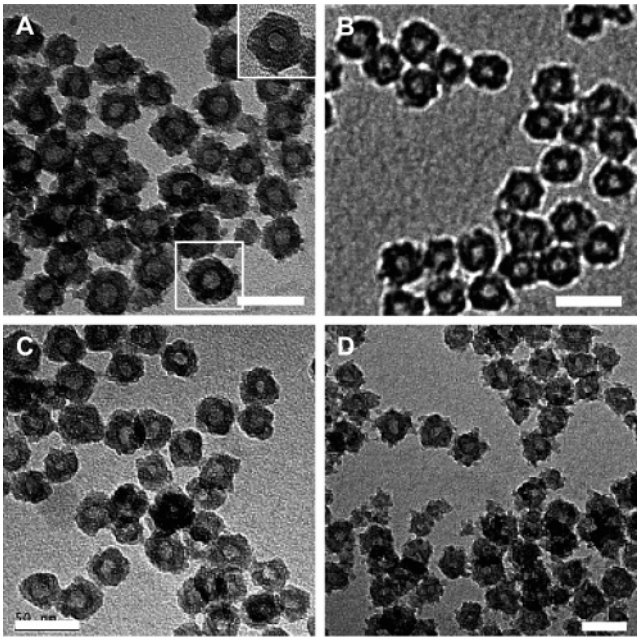

Figure 5. TEM images obtained for the following: (A) hybrid copolymer−silica particles prepared by mixing 2.0 mL of a 0.25 w/v % aqueous solution of partially quaternized shell cross-linked (SCL) micelles [30% target degree of shell cross-linking for the PDMA chains] solution with 2.0 mL of TMOS for 40 min (the upper inset in A shows a representative hollow silica particle after pyrolysis of the copolymer component by calcination at 800 °C; the lower inset highlights a typical core−shell copolymer−silica particle prior to calcination); (B) hybrid copolymer−silica particles formed using partially quaternized SCL micelles (50% target degree of shell cross-linking with respect to the PDMA chains) using the same conditions as those employed in (A); (C) hybrid copolymer−silica particles formed 40 min after stirring an initially homogeneous solution comprising 2.0 mL of a 0.25 w/v % aqueous solution of partially quaternized SCL micelles [30% target degree of shell cross-linking for the PDMA chains], 2.0 mL of TMOS, and 2.0 mL of methanol; (D) hybrid copolymer−silica particles formed 120 min after stirring using the same conditions as those described in (C). The scale bars are 50 nm in each case.

inorganic cross-linking of copolymer micelles: Huo et al. recently utilized nonionic block copolymers as micellar templates for silica deposition.[12] However, these nonionic block copolymers catalyze in situ silica deposition at low pH (0.85 M HCl), rather than the neutral pH conditions employed in the present study. Such acidic conditions are unsuitable for our $PDPA_{23}$−$PDMA_{68}$ diblock copolymer, since this precursor does not form micelles at low pH. Moreover, it was necessary for Huo et al. to use a relatively expensive reagent (diethoxydimethylsilane) to control the extent of silica deposition in order to obtain colloidally stable copolymer−silica particles. This restriction does not apply to the present study.

We also investigated the use of *preformed* SCL micelles as templates for silica deposition. Thus the coronal PDMA chains of micelles were selectively quaternized (and simultaneously cross-linked) at a target degree of cross-linking of 30 mol % using 1,2-bis(2-iodoethoxy)ethane (BIEE), as described by Bütün and co-workers.[14] DLS studies conducted at 25 °C indicated an intensity-average micelle diameter of 37 nm for the cationic SCL micelle precursors at pH 7. Silica deposition was performed under the same conditions as those employed for noncross-linked micelles. Figure 5A shows a typical TEM image of the resulting hybrid copolymer−silica particles. Their intensity-average and number-average diameters from DLS and TEM are 35 and 32 nm, respectively, which are in reasonably good agreement with the values obtained for the SCL micelle precursor. Furthermore, their core−shell morphology is also clearly evident. For example, the individual particle indicated by the white square in Figure 5A has a PDPA core of approximately 14 nm and a silica/PDMA mixed shell thickness of around 11 nm. Thermogravimetric analyses indicated that the mean copolymer content of these copolymer−silica particles was about 19% by mass. Silica deposition onto SCL micelles prepared at a target degree of cross-linking of 50% produced similar results, as shown in Figure 5B. Compared to the copolymer−silica particles prepared using noncross-linked micelles under similar conditions (see Figure 2B), the copolymer−silica particles obtained from SCL micelles have larger cores and thinner shells. Moreover, there is no evidence for nontemplated silica within the dispersion, indicating that silica deposition is again well-controlled. Silica deposition experiments were also performed at lower levels of TMOS. On mixing a 2.0 mL aliquot of a 0.25 w/v % copolymer micelle solution (50% target degree of cross-linking using BIEE) with 58 mg of TMOS for 20 min, silica deposition led to aggregation, rather than a colloidally stable dispersion. TEM studies indicated the formation of copolymer−silica particles of about 17−20 nm, as well as interconnected, fused primary particles (see Figure S3A). Thermogravimetric analyses indicated a mean copolymer content of around 30% by mass, indicating a silica conversion of approximately 50%. However, the formation of copolymer−silica particles was much improved by using a slight excess of TMOS under the same conditions. Thus mixing 2.0 mL of a 0.25 w/v % copolymer micelle solution (50% target degree of crosslinking using BIEE) with 116 mg of TMOS for 20 min produced a colloidally stable dispersion, as judged by visual inspection. As shown in Figure S3B, copolymer−silica particles with a number-average diameter of about 20−25 nm were obtained. Thermogravimetric analyses indicated a mean copolymer content of about 24% by mass, indicating a silica conversion of around 35%.

Silica deposition can be also controlled using SCL micelles under initially homogeneous conditions. A 2.0 mL aliquot of a 0.25 wt % SCL micelle solution was added to a mixture of 2.0 mL of methanol and 2.0 mL of TMOS. The methanol acts as a cosolvent and ensures that the TMOS is miscible with the aqueous phase. After silica deposition for 40 min, TEM studies confirmed the formation of well-defined hybrid copolymer−silica particles, as expected (Figure 5C). Even after 120 min, there is no evidence for nontemplated silica nanostructures (Figure 5D). The SCL micelle-derived copolymer−silica particles shown in Figure 5A were further characterized using FT−IR spectroscopy and aqueous electrophoresis. FT−IR studies confirmed silica formation, since bands were observed at 1080, 950, 800, and 470 cm^{-1} for these hybrid copolymer−silica particles due to the inorganic component; these bands were absent in the spectra obtained for the copolymer micelles prior to silica deposition (see Figure S4). After calcination at 800 °C, the characteristic bands at 1726 cm^{-1} due to the pyrolyzed copolymer completely disappeared, while those bands assigned to the thermally stable silica were still observed (see Figure S4). TEM studies indicated that the calcined hybrid copolymer−

(29) Perkin, K. K.; Turner, J. L.; Wooley, K. L.; Mann, S. *Nano Lett.* **2005**, *5*, 1457−1461.

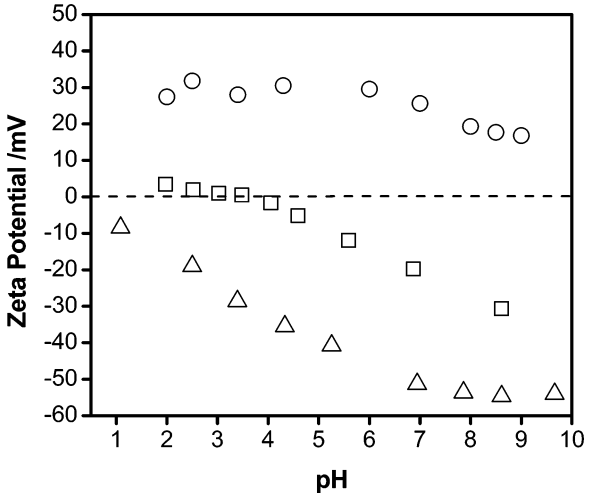

Figure 6. Zeta potential vs pH curves obtained for the original shell cross-linked (SCL) micelles prepared from the $PDPA_{23}$−$PDMA_{68}$ diblock copolymer at a target degree of cross-linking of 30% for the PDMA coronal chains (○) and the final hybrid copolymer−silica particles synthesized after mixing 2.0 mL of a 0.25 w/v % SCL micelle solution (target degree of cross-linking = 30%) with 2.0 mL of TMOS for 40 min (□). For comparative purposes, the zeta potential curve obtained for an ultrafine commercial 20 nm silica sol (Nyacol 2040) is also shown (△).

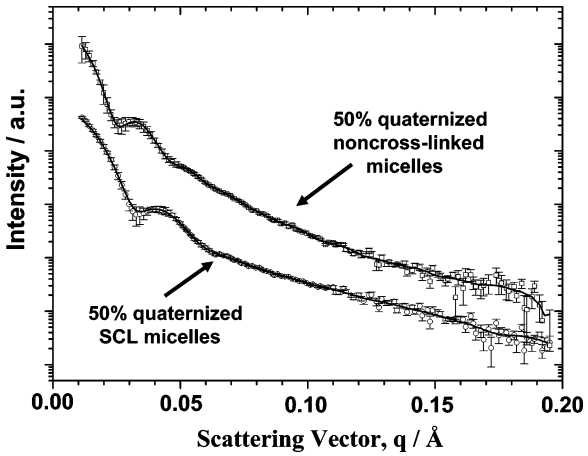

Figure 7. The q dependence (where q is given by $q = 4\pi \sin \theta/\lambda$, where θ is half the scattering angle and λ is the X-ray radiation wavelength) of the scattered intensity obtained by SAXS from dilute aqueous dispersions of hybrid copolymer−silica particles ((<0.50 vol %) synthesized using 50% quaternized shell cross-linked micelles and 50% quaternized noncross-linked micelles, respectively) and the corresponding intensities computed by the regularization technique using the GNOM computer program (solid lines). For clarity, the lower SAXS pattern has been reduced by a scaling factor of 10.

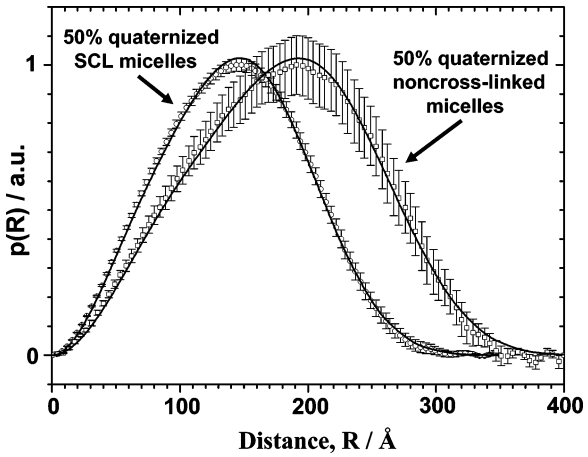

Figure 8. Distance distribution functions of the hybrid copolymer−silica particles synthesized from shell cross-linked and noncross-linked micelles (○ and □, respectively) calculated from the SAXS patterns shown in Figure 7. These $p(r)$ curves were normalized and fitted using a core−shell model (solid lines) assuming a normal distribution for the overall particle radius. See Supporting Information for further details of this data analysis.

silica particles formed nanosized hollow silica particles after pyrolysis of the organic component (see inset of Figure 5A).

Zeta potential measurements also supported the deposition of silica within the coronal layer of these micelles (see Figure 6). The precursor SCL micelles (30% target degree of cross-linking for the PDMA chains) had positive zeta potentials over the whole pH range investigated due to their cationic PDMA shells. However, the copolymer−silica particles exhibited negative zeta potentials over a wide pH range, with an isoelectric point at around pH 3.3. This latter behavior is similar to that found for aqueous colloidal silica sols[30] (see Figure 6) and is therefore consistent with the SCL micelles becoming coated with an overlayer of silica. The difference between the electrophoretic curves obtained for the silica sol control and the hybrid copolymer−silica particles most likely reflects the cationic nature of the partially quaternized PDMA chains, which may well protrude beyond the silica shell.

SAXS patterns (see Figure 7) of dilute aqueous colloidal dispersions of copolymer−silica particles prepared from two types of $PDPA_{23}$−$PDMA_{68}$ copolymer micelles (50% quaternized noncross-linked micelles and 50% SCL micelles prepared using MeI and BIEE, respectively) each show well-defined first and second minima, with some evidence of a third minimum for the noncross-linked micelles. Assuming a spherical particle morphology, these SAXS curves suggest that the polydispersity (σ) of the overall particle radius is about 20% and 15% for the shell cross-linked and noncross-linked micelles, respectively. The distance distribution functions [$p(r)$] calculated from these SAXS curves (see Figure 8) are similar to the $p(r)$ data previously reported for spherical particles.[19] A core−shell model described by the following parameters was used to fit the $p(r)$ functions: electron density of the core ξ_c, electron density of the shell ξ_s, electron density of the surrounding media ξ_m, the particle core radius R_c, and the overall particle radius R_s, including its polydispersity as represented by a normal distribution of the overall particle radius (see Supporting Information for further details). Good fits were obtained (see Figure 8) with the extracted geometrical parameters (R_c and R_s) correlating reasonably well with the corresponding TEM images obtained for these copolymer−silica particles. For example, a silica shell thickness t (where $t = R_c - R_s$) of 5.6 nm was calculated for the copolymer−silica particles obtained from the 50% SCL micelles, whereas TEM studies indicated an estimated silica shell thickness of around 6 nm. Similarly, a silica shell thickness of 8 nm was calculated for the copolymer−silica particles prepared using the 50% noncross-linked micelles, whereas TEM suggested a shell thickness of around 11 nm. In this latter case, it is perhaps noteworthy that a somewhat less reliable fit (i.e., with larger error bars) was obtained for the distance distribution function shown in Figure 8.

Finally, the deposition of gold nanoparticles within these copolymer−silica particles was attempted. First $HAuCl_4$ was

(30) Percy, M. J.; Armes, S. P. *Langmuir* **2002**, *18*, 4562−4565.

used to protonate the weakly basic PDPA chains within the cores of the copolymer−silica particles. Then the $AuCl_4^-$ counterions associated with the protonated PDPA chains were reduced in situ to produce zerovalent gold nanoparticles using $NaBH_4$ as a reducing agent.[31] The color of the dispersion changed from white to wine red after the reduction step, indicating the formation of nanosized gold sols.[31,32] TEM observations (see Figure S5) supported the generation of gold sols within the cores of the copolymer−silica particles, although some disruption of the silica shells is also apparent. Thus this experiment also provides good evidence for the PDPA chains being located within the cores of the copolymer−silica particles. It may be possible to encapsulate other species such as quantum dots or biologically active molecules; we intend to address this possibility in future work. Due to their well-defined nanostructures, these copolymer−silica particles may have potential applications in biolabeling, biodiagnostics, drug delivery, and imaging.[23]

Conclusions

Cationic diblock copolymer micelles have been used as colloidal templates for the deposition of silica at ambient temperature and neutral pH. Partial (and selective) quaternization of the 2-(dimethylamino)ethyl methacrylate residues on the copolymer chains leads to the formation of hybrid copolymer−silica particles with well-defined core−shell morphologies, with the core comprising pH-responsive poly(2-(diisopropylamino)-ethyl methacrylate) chains and the shell comprising both silica (major component) and partially quaternized poly(2-(dimethylamino)ethyl methacrylate) chains. ^{1}H NMR studies indicate that the core chains can be protonated, and aqueous electrophoresis studies confirm that these hybrid copolymer−silica particles have silica-rich surfaces. SAXS studies allow calculation of mean wall thicknesses for the silica−polymer shell that are in good agreement with thicknesses estimated by TEM. Finally, silica deposition stabilizes these copolymer micelles under conditions that would otherwise cause micelle dissociation (e.g., low pH). Thus inorganic silicification can be considered as a convenient alternative to organic cross-linking for the synthesis of shell cross-linked micelles in aqueous solution.

Acknowledgment. Dr V. Bütün is thanked for the synthesis of the $PDPA_{23}$−$PDMA_{68}$ diblock copolymer. Mr. Andreas Schmid and Dr. Jianzhong Du are thanked for their help with the TEM studies. EPSRC is acknowledged for a postdoctoral fellowship for J.-J.Y. (Platform grant, GR/S25845). S.P.A. is the recipient of a 5-year Royal Society Wolfson Research Merit Award.

Supporting Information Available: Full experimental details for synthesis protocols and characterization techniques; TEM images of hybrid copolymer−silica particles obtained using micelles with 100% quaternized PDMA chains as templates, particles after treatment by dispersing in water at pH 2, hybrid copolymer−silica particles obtained using SCL micelles (50% mean target degree of cross-linking) at a reduced TMOS concentration and also gold sol-loaded nanoparticles; FT−IR spectra for the SCL micelles and corresponding hybrid copolymer−silica particles. This material is available free of charge via the Internet at http:// pubs.ac.org.

JA0674946

(31) (a) Liu, S.; Weaver, J. V. M.; Save, M.; Armes, S. P. *Langmuir* **2002**, *18*, 8350−8357. (b) Du, J.; Tang, Y.; Lewis, A. L.; Armes, S. P. *J. Am. Chem. Soc.* **2005**, *127*, 17982−17983.
(32) Wilcoxon, J. P.; Williamson, R. L.; Baughman, R. *J. Chem. Phys.* **1993**, *98*, 9933−9950.